JOURNAL OF MATERIALS SCIENCE 27 (1992) 6098–6104

Calorimetric and other studies of intermetallic phase formation in Ag/Al bilayer thin films

R. ROY, S. K. SEN
Department of Materials Science, Indian Association for the Cultivation of Science, Jadavpur, Calcutta 700 032, India

Silver and aluminium bimetallic thin film couples have been studied using constant heating rate differential scanning calorimetry both on cleaned glass substrates and freshly cleaved NaCl crystals. The most striking feature was the occurrence of two maxima in the reaction rate during the formation of a single product phase, Ag_2Al, suggesting a two-step growth process. The activation energy for this reaction was 0.98 eV in the first step and 0.93 eV in the second step. These values are in good agreement with values obtained by a different technique, i.e. Rutherford back-scattering. Transmission electron microscopy, thin film X-ray diffraction, the change in resistance of bilayer films with temperature and thermodynamic and kinetic analyses have been used to investigate the intermetallic phase formation. It was observed that substrate plays an important role in the kinetics of thin-film reaction.

1. Introduction

Interactions between thin films occur at a temperature much lower than the corresponding reactions of well-annealed bulk specimens because the interface constitutes a major fraction of the total volume compared with the bulk specimen. As surface diffusion and diffusion along grain boundaries or defects play a major role, study of the kinetics of this interaction is always important. There are various direct and indirect methods to follow this reaction.

Although experimental techniques such as Auger electron spectroscopy, ion back-scattering, secondary-ion mass spectroscopy and X-ray photoelectron spectroscopy, etc., can characterize the nature and degree of interfacial reactions, they cannot monitor such reactions continuously. The measurement of electrical resistance (contact or composite) [1] of a bimetallic sample is a method which circumvents such problems. Recently, differential scanning calorimetry (DSC) has also been used to provide an insight into the thermodynamics and kinetics of several such interfacial reactions in multilayer films, namely, the formation of amorphous alloys at the interface [2], formation of intermetallic compounds at the interface [3] and reaction in multilayers of nickel and amorphous silicon [4].

In the present work, we chose the system Ag/Al for such study. Generally, the most studied materials are those in the reactions of aluminium films with gold, hafnium and chromium which are used in integrated circuit metallization structures. Ag/Al is a similar system but much simpler than Au/Al, where five intermetallic phases are formed below 773 K. From a previous study [5], where only one phase (Ag_2Al) has been identified, it seems that this should be a suitable system to be studied using DSC. The DSC measurements can also be confirmed by *in situ* measurement of electrical resistivity, and phase identification at different stages of temperature treatment can be made using X-ray diffractograms (XRD). Lastly, the samples have been examined using transmission electron microscopy (TEM) where the microstructural changes on annealing could be studied in thin films deposited on different substrates.

2. Experimental procedure

Bilayer films of silver and aluminium were prepared by sequential evaporation from elemental sources on freshly cleaned glass substrates and freshly cleaved NaCl salt under a vacuum of the order of 70 μPa. Henceforth, in the text, unless mentioned otherwise, the discussions will refer to the films on glass substrates. The thickness of the bilayer films for different experimental observations are shown in Table I. Z_{max} shown in Table I corresponds to the reaction length for Ag_2Al formation, such that the overall composition ratio of silver and aluminium becomes 2:1. For example, for the first film, 65 nm Ag reacts with approximately 33 nm Al so that Z_{max} is 98 nm, whereas the total thickness is 120 nm leaving behind 22 nm of unreacted aluminium. Films deposited were subsequently removed from the substrate and thermal analyses were performed using a Perkin–Elmer DSC7 power-compensated differential scanning calorimeter. About 2 mg of sample was used for each DSC run. The experiments were performed in constant heating rate mode in a nitrogen atmosphere to prevent oxidation, the starting temperature for all the runs being 322 K. In all cases, the sample was first allowed to stabilize at 322 K and then heating was initiated. The experiment was performed on two film thicknesses, as shown in

0022–2461

TABLE I Description of bilayer films used in this experiment. The reactant layer thicknesses are for as-deposited films, while the product layer thicknesses, Z_{max}, are calculated from the stoichiometry of product phase and from the amount of reactants available

Film	Reactant layer thickness (nm)		Investigation done	Z_{max} (nm)
	Ag	Al		
1	65	55	DSC (on glass and NaCl)	98
2	95	100	DSC, electrical resistivity	142
3	120	90	XRD	180
4	50	50	TEM	75

Table I, at a constant heating rate, i.e. 20 K min^{-1}. However, for the first film, the heating rate was varied from 2–40 K min^{-1}.

Simultaneously, *in situ* measurements of the change in electrical resistivity with temperature of the bilayer film sandwich (film 2, Table I) were performed. The detailed experimental apparatus has been described earlier [1]. A constant heating rate of about 2 K min^{-1} was applied and the change in resistance was automatically recorded in a microvolt amplifier recorder. A suppression unit, which suppresses part of the voltage drop, was used and the residual voltage after suppression was amplified and displayed as a function of time in a recorder. A constant current source (Keithly model 224) and a nanovoltmeter (Keithly model 181) were used for frequent checking of the recorded data. Arrangements for heating the substrates were incorporated using a substrate heater controlled by a proportional type of temperature controller. The sample temperature was measured accurately with a copper–constantan thermocouple having intimate contact with the substrate.

XRD studies were performed on films of about 120 nm Ag and 90 nm Al, both as-deposited and annealed at different temperatures, and the diffraction patterns were chart-recorded with a Philips X-ray diffractometer model (model PW 1050, 51) using monochromatic LiF filtered CuK_α radiation.

The specimens for examination by TEM were prepared by first depositing about 50 nm Ag and then about the same thickness of aluminium, both on freshly cleaned glass substrates and NaCl crystals. These films were next floated off in deionized water and removed on to a copper grid for subsequent annealing at 523 K for 1 h and then examined in a 200 kV Philips (Jeol) microscope.

3. Results and discussion

3.1. Phase identification using XRD

The XRD patterns of Ag/Al bilayered films subjected to isochronous annealing for 1 h at a temperature between room temperature and 473 K, are shown in Fig. 1. The as-deposited film and the film annealed at 373 K (not shown) contain only not fully resolved peaks of silver and aluminium, whereas the film annealed at 423 K reveals the spectrum modification.

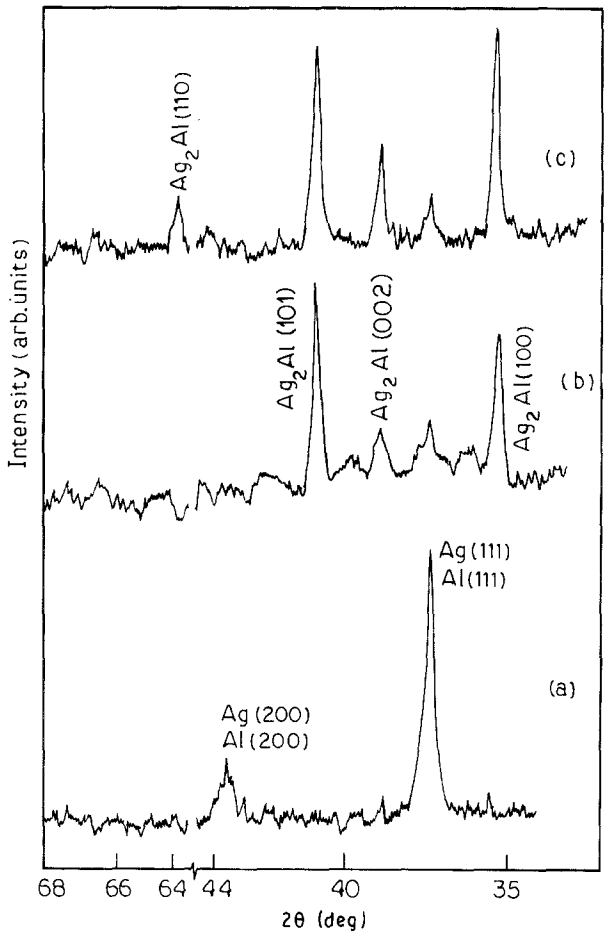

Figure 1 X-ray diffractogram of Ag/Al film with silver at the bottom and aluminium at the top, deposited on cleaned glass substrates: (a) unannealed; and annealed at (b) 423 K for 1.5 h, (c) 473 K for 1 h.

Silver and aluminium films react to form Ag_2Al intermetallic compound. Further annealing at higher temperature gradually increases the intensity of the Ag_2Al peaks, therefore it can be inferred that the intermetallic compound formation starts above 373 K. The increase in intensity of the Ag_2Al peak with annealing might be due to microstructural refinement of the Ag_2Al layer, as well as the formation of additional Ag_2Al.

3.2. Differential scanning calorimeter curves

The calorimeter curves for films of two different thicknesses heated at a constant rate (20 K min^{-1}) are shown in Fig. 2. The heat flow, H, per unit time indicated along the vertical axis of the figure is proportional to the reaction rate, i.e. volume of the new phase, V i.e.

$$\frac{dH}{dt} \propto \frac{dV}{dt} \quad (1)$$

The horizontal axis which represents the sample temperature, is also proportional to the time during constant heating experiments. Two minima corresponding to the negative heat of reaction are observed. As the film thickness changes from 120 nm (dotted curve Fig. 2) to 195 nm (solid curve Fig. 2), the peak heights are decreased. The Peak 1 position does not appreciably change with thickness, but Peak 2 shifts to higher

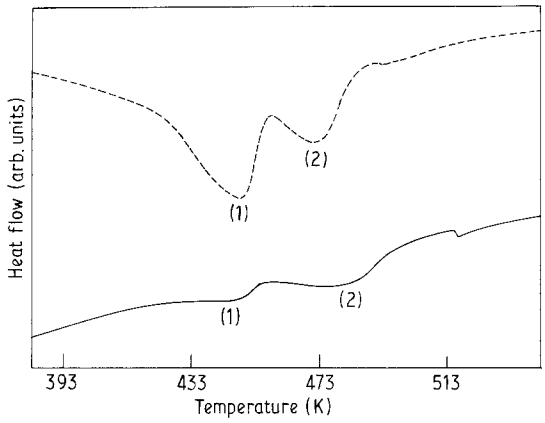

Figure 2 Differential scanning calorimetry curves of Ag/Al films heated at 20 K min^{-1}; layer thickness Z_{max}, (· · ·) 98 nm and (——) 142 nm. (1, 2) Two peak minima, see text.

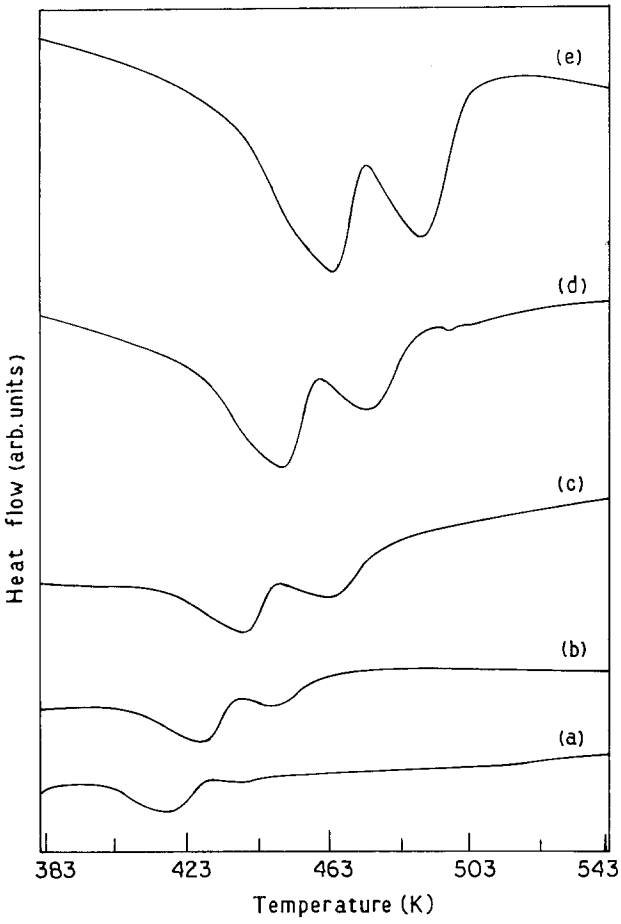

Figure 3 DSC traces of 65 nm Ag/55 nm Al films deposited on glass slides for heating rates (K min^{-1}): (a) 2, (b) 5, (c) 10, (d) 20 and (e) 40.

temperature with thicker reactant layers. DSC traces of the film 120 nm thick have also been obtained for five different heating rates of 2–40 K min^{-1} (Fig. 3). Upon increasing the heating rate in DSC scans, both peaks are observed to occur at progressively higher temperature, indicating that the interaction process is thermally activated. This shift with increasing scanning rate can be related to the activation energy of the reaction using the following expression developed by Kissinger [6]

$$\ln(H/T_p^2) = C_2 - Q/kT_p \qquad (2)$$

where H is the heating rate, T_p the peak temperature,

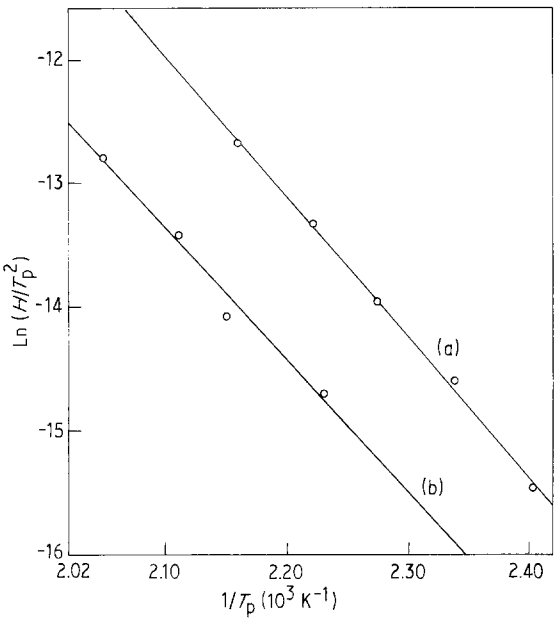

Figure 4 Kissinger plot for 65 nm Ag/55 nm Al bilayer films deposited on glass slides: (a, b) Peaks 1 and 2, respectively.

C_2 a constant, k the Boltzmann constant, and Q the activation energy of reaction.

In Fig. 4, $\ln(H/T_p^2)$, as observed from Fig. 3, has been plotted against $1/T_p$. From a least square fitting of the data it is observed that Q for Peaks 1 and 2 are 0.98 and 0.93 eV, respectively. As the position of Peak 2 for the scanning rate of 2 K min^{-1} is uncertain, this has been omitted for the corresponding Q calculation.

The use of DSC for studying phase formation is well known. It is possible to obtain kinetic data on the phase transformation from the study of the shape of transformation peaks as well as their shifts with scanning rate. Recently this techique has been used by Clevenger and co-workers [3, 7] to analyse amorphous silicon thin-film reactions. In our case, two extremes occur in the reaction rate during the formation of a single product phase. The first extreme can be interpreted as being due to the inhomogeneous formation of the product phase at the initial reactant layer interface by nucleation at many locations. Here the interfacial area, rather than the layer thickness, is being consumed. But with time, the interfacial area is reduced and the continuous product layer is formed. Hence the second extreme corresponds to completion of the reaction due to the consumption of one or both reactant layers.

Assuming the existence of cylindrical nucleation sites of areal density n, initial height Z_0, and radius r, in the plane of interface, the nuclei grow radially in the early stage to cover the initial interface plane completely. The growth rate of the nuclei can be modelled as

$$\frac{dr}{dt} = K_{i0} \exp(-Q_i/kT) \qquad (3)$$

where K_{i0} and Q_i are the interface-limited pre-exponential factor and activation energy, respectively. If R is the scanning rate, defined by $R = dT/dt$, then r can

be expressed as

$$r = \frac{K_{i0}}{R}\int_{T_0}^{T}\exp(-Q_i/kT) \quad (4)$$

The position of the first extreme will depend upon the time it takes for the radial growth of cylinders to meet one another in the initial interface. If there are n cylinders per unit area, then the extended area fraction which would react is $n\pi r^2$. But after an initial period of time, the reaction rate will be reduced due to the impingement of one growing cylinder upon another. So, for randomly oriented nucleation sites, a Johnson–Mehl [8] and Avrami [9–11] type of analysis can be used to obtain the actual reacted area fraction

$$X_A = 1 - \exp(-n\pi r^2) \quad (5)$$

so the first extreme corresponds to the termination of interface-limited growth.

Assuming the diffusion-controlled thickening of the product layer for the second extreme, the growth rate can be described by

$$\frac{dZ}{dt} = \frac{K_{d0}}{Z}\exp(-Q_d/kT) \quad (6)$$

where K_{d0} and Q_d are the corresponding prefactor and activation energy, respectively. Q_i and Q_d have been found to be 0·98 and 0.93 eV, respectively (Fig. 4). If Z_0 is the thickness of the Ag_2Al phase when it first nucleates at the interface at a corresponding temperature, T_0, the thickness, Z, at any temperature, T, is given by

$$Z^2 - Z_0^2 = \frac{2K_{d0}}{R}\int_{T_0}^{T}\exp(-Q_d/kT)\,dT \quad (7)$$

The shift in Peak position 2 with the increase in film thickness can now be understood in terms of the above model. Combining the results of the two mechanisms, the product phase growth can be described by a single model which gives the reaction rate in terms of the volume fraction, X_v, as

$$\frac{dX_v}{dt} = \left(\frac{dX_A}{dt}\right)\left(\frac{Z}{Z_{max}}\right) + X_A\left(\frac{dZ}{dt}\right)\left(\frac{1}{Z_{max}}\right) \quad (8)$$

where

$$\frac{dX_A}{dt} = 2n\pi r\left(\frac{dr}{dt}\right)\exp(-n\pi r^2) \quad (9)$$

Now Z_0 can be found out from the area or height of the two peaks corresponding to a particular film thickness. Then K_{d0} is determined from the layer thickness dependence of the second extremum, i.e. from Equation 7. The composite parameter, nK_{i0}^2, is determined for both the films having different thicknesses by fitting the position of Peak 1. These are 1.2×10^{19} and $3.1 \times 10^{19}\ s^{-2}$ for films 1 and 2, respectively, from which the average value of nK_{i0}^2 can be taken as $2.1 \times 10^{19}\ s^{-2}$. All these parameters are shown in Table II. nK_{i0}^2 is proportional to the nucleation site density, n, and should change slightly with the thickness of the films. But K_{i0}^2 may not be absolutely constant. Thus, in this case, from the variation of composite parameter with thickness, we cannot conclude anything about the corresponding change in nucleation site density, n.

TABLE II Values of the model parameters used to describe the reaction kinetics of Ag/Al bilayer systems

Z_0 (nm)	nK_{i0}^2 (S^{-2})	Q_i (eV)	K_{d0} ($cm^2 S^{-1}$)	Q_d (eV)
50	2.1×10^{19}	0.98	10^{-2}	0.93

This method has been previously applied to nickel/amorphous silicon (Ni/a – Si) and niobium/aluminium (Nb/Al) thin-film systems [3]. In both these cases the activation energies Q_i and Q_d were found to be same, i.e. 1.5 eV. For the Ni/a–Si system, this value of activation energy seems to be in good agreement with experiments performed by other methods, e.g. Rutherford back-scattering studies [12] (RBS). There seems to be no independent check for the Nb/Al system so far. For our system, there are slight differences in Q_i and Q_d values. So far there are two quoted values in the literature for the activation energy of formation of Ag_2Al phase. Weaver and Brown [13] using optical reflectivity and TEM techniques, deduced $Q = 1.15$ eV upto 513 K for air anneal. Baglin *et al.* [5] studied the kinetics of Ag_2Al formation in the temperature range 373–493 K using RBS. The overall activation energy was found to be 0.86 ± 0.05 eV which is slightly lower than our estimated value. However, it seems to be closer to the grain-boundary self-diffusion value in silver (0.9 eV) rather than that in aluminium (0.6 eV). Thus it seems that the growth of the Ag_2Al layer is mainly due to the grain-boundary diffusion of aluminium in silver or Ag_2Al itself. Nevertheless, the interaction model, as envisaged in the DSC experiment, is in agreement with Baglin's observation using a different tool (i.e. RBS) to observe this phenomenon. He observed that although silver might diffuse through the aluminium grain boundary, silver could not be traced within the aluminium grains. Nucleation of Ag_2Al phase takes place at the interface plane, most likely at the junction of grain boundaries of the silver film. Further growth of Ag_2Al phase is governed by the diffusion of aluminium along Ag/Ag_2Al boundaries.

Thus the calorimeter experiment precisely detects the nucleation at the interface and subsequent propagation of product phase through grain boundaries and the grain interior possibly of silver.

3.3. Effect of substrate

The calorimeter experiment was performed on bilayer films deposited on salt and subsequently removed by dissolution in water and dried. The DSC plot of such a film of thicknesses 65 nm Ag and 55 nm Al is shown in Fig. 5. It can be seen that the peak heights are much smaller and peak positions especially of Peak 1 have been shifted to higher temperatures compared to the corresponding film deposited on glass (Fig. 2). For comparison, both the films have been heated at the

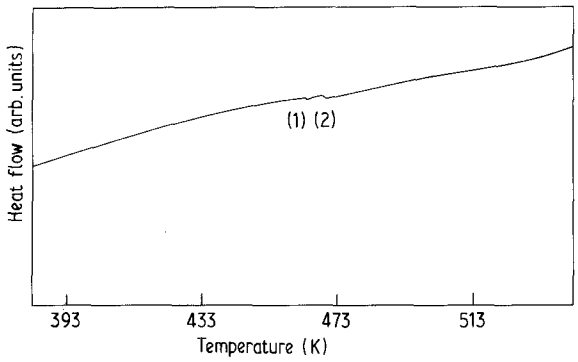

Figure 5 DSC traces of 65 nm Ag/55 nm Al film deposited on NaCl heated at 20 K min^{-1}.

same rate (i.e. 20 K min^{-1}) and drawn on the same scale.

Peak 1 has been interpreted as being due to the inhomogeneous formation of the product phase at the initial reactant layer interface by nucleations at many locations. Therefore a shift to higher temperature or decrease in peak intensity means that few nucleation sites are formed along the film interface deposited on salt. It is shown that the presence of an impurity at the interface can block the interfacial reaction [14]. So the above phenomenon might be thought of as due to contamination of the salt at the interface inspite of thorough rinsing of the salt with water. However, recently, it was observed by Ma *et al.* [15] that impurities play no significant role in the Al/Ni system deposited under ultra-high vacuum (UHV) conditions and non-UHV samples. Moreover, the salt has to diffuse through the silver film before contaminating the interface. It was also observed by Ma *et al.* [15] that nucleation site density strongly depends on the film microstructure, especially the grain size of the reactant layers. According to their suggestions, certain types of granular defects, such as grain-boundary triple junctions, can act as heterogeneous nucleation sites for the new compound phase. Because the microstructure and grain size of the films deposited on salt are different from those on glass substrates, the above phenomenon can be qualitatively explained assuming grain size is much larger for samples deposited on salts than on glass slides. The effect of substrate has been further observed in the subsequent measurements on electrical resistivity and TEM.

3.4. Measurement of change in resistance of Ag/Al couple with temperature

In order to check the effect of the growth of a particular phase with temperature, the temperature dependence of electrical resistivity of a Ag/Al couple was carefully monitored and recorded. The experiment was performed both on well-cleaned and baked glass substrate and freshly cleaved NaCl substrate. On the glass substrate, a silver film about 95 nm thick, was first vacuum deposited, heated to 520 K for 0.5 h to anneal out defects, cooled to room temperature and then aluminium films, about 100 nm thick were vacuum evaporated on it. The sample was next heated inside the deposition unit without breaking the

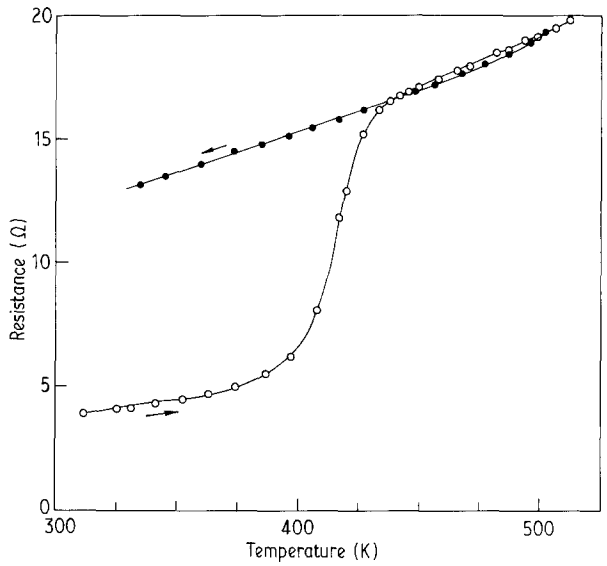

Figure 6 Resistance against temperature plot of 95 nm Ag/100 nm Al film deposited on cleaned glass substrate.

vacuum at a constant rate of 2 K min^{-1}. The experiment was repeated on freshly cleaved NaCl substrate, where the deposited films were almost of the same thickness as those on the glass substrate, but the heating rate was much faster (approximately 30 K min^{-1}) in order to minimize any possible effect of diffusion from the substrate. The resistivity–temperature graphs on glass and NaCl substrates are plotted in Figs 6 and 7, respectively. It can be seen from Fig. 6 that an otherwise smoothly rising curve sharply increases from 400 K and continues up to 430 K, and then maintains almost the same temperature variation as in the beginning up to 520 K. The subsequent cooling curve follows almost the same TCR as was observed at the beginning or end of the heating curve. The resistivity experiment performed on salt substrate, on the other hand, does not show such a pronounced effect with temperature (Fig. 7) except for a plateau around the same temperature range.

From the resistivity–temperature plot on the glass substrate (Fig. 6) it is evident that resistivity increases rapidly with the formation of Ag_2Al phase between 400 and 430 K, the mean of which is 415 K. This is almost the same as that observed from DSC experiment. While the formation of Ag_2Al phase was clearly manifested during heating of the as-deposited bilayer films on the glass substrate, that on the NaCl substrate (Fig. 7) failed to detect such changes. However, we could observe a plateau around the same temperature range which can be associated with the formation of Ag_2Al precipitation. This indicates that the substrate plays a major role on the kinetics of thin-film reactions.

3.4. Characterization of microstructure using TEM

The electron micrographs and SAD patterns of several Ag/Al bilayer films deposited on NaCl salt and cleaned and baked glass slides were studied. All films

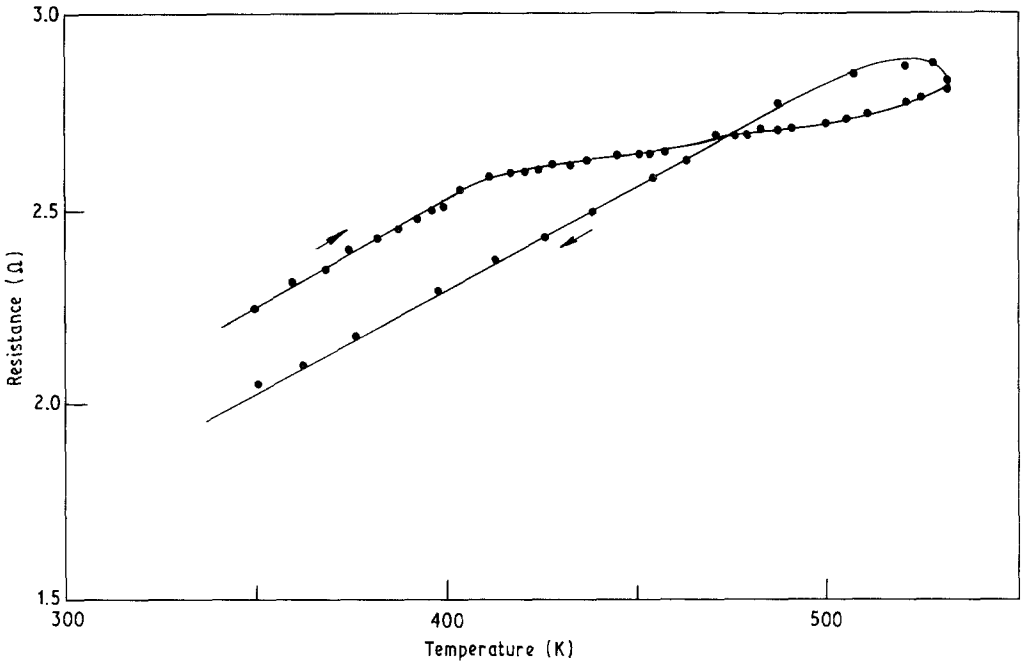

Figure 7 Resistance–temperature plot for the film of same thickness as in Fig. 6, deposited on freshly cleaved NaCl.

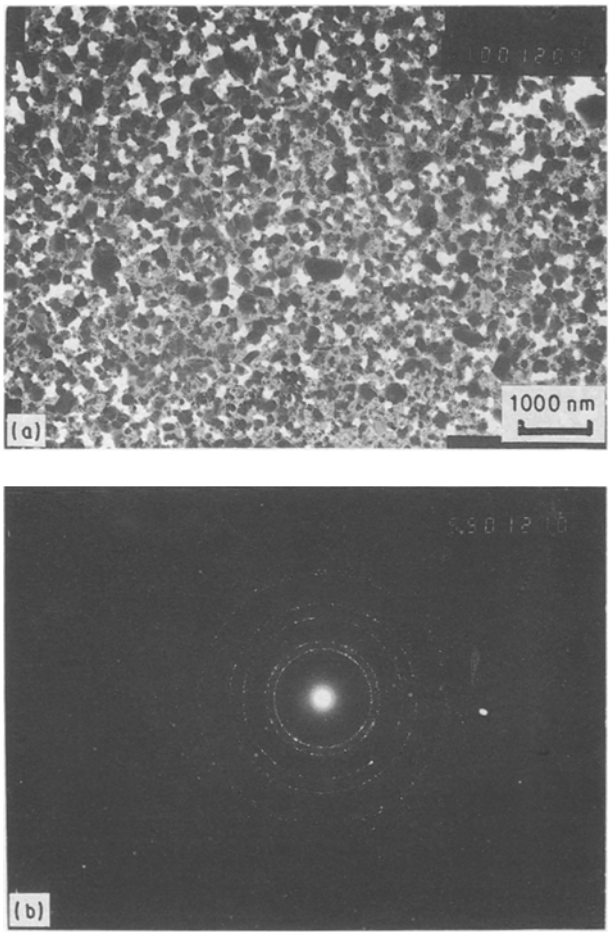

Figure 8 Transmission electron micrographs of annealed (523 K for 1 h) Ag/Al films deposited on NaCl salt: (a) microstructure, (b) SAD pattern.

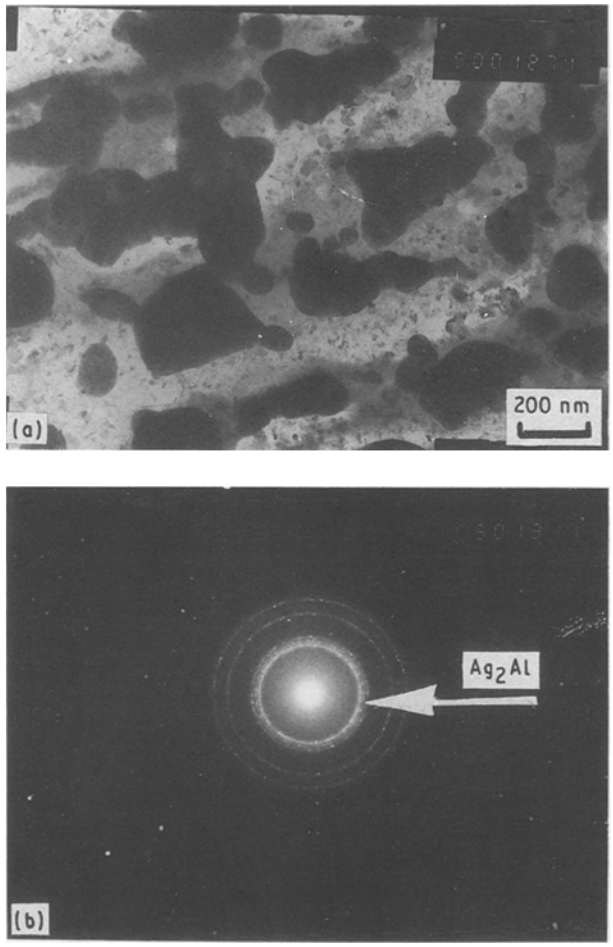

Figure 9 Transmission electron micrographs of annealed (523 K for 1 h) Ag/Al film deposited on cleaned glass substrate: (a) microstructure, (b) SAD pattern.

were subsequently mounted on copper grids and annealed at 523 K for 1 h. We could observe a considerable difference in the micrographs and the diffraction patterns of the films on salts and glass slides. The micrograph of the bilayer annealed film deposited on salt (Fig. 8a) shows grains of silver and aluminium having an average grain size of about 250 nm. The corresponding diffraction pattern (Fig. 8b) does not

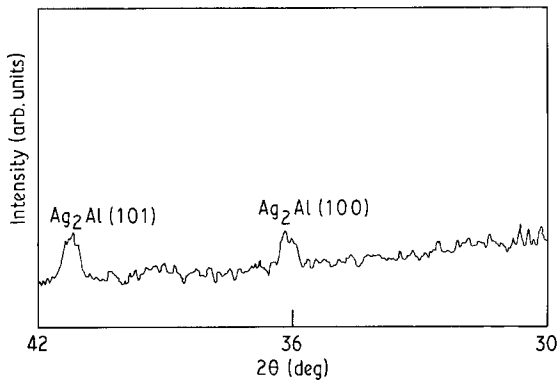

Figure 10 X-ray diffractogram of Ag/Al film deposited on glass substrate and annealed simultaneously with the TEM specimen.

indicate the growth of intermetallic phases. The grains of the unannealed film (not shown) are almost twenty times smaller. However, a specimen annealed on a cleaned glass slide shows the presence of smaller particles of grain size about 20 nm with some larger agglomerated grains (Fig. 9a). The smaller black particles are Ag_2Al precipitates which can be seen from the corresponding selected-area diffraction pattern (Fig. 9b) and confirmed from the XRD pattern of another sample deposited and annealed simultaneously with the TEM specimen (Fig. 10). The precipitation of Ag_2Al phase can be compared with a similar phenomena of precipitation of θ-phase along Al/Cu grain boundaries [16]. The TEM observations support our earlier conclusion from the DSC experiment, that the grain size and microstructure of the reactant layers play a significant role in compound phase formation at the interface.

4. Conclusion

From the discussion it can be concluded that in order to understand the mechanism of reactions at the interface, their reactions and thermodynamics, DSC is one of the simplest and quickest techniques. However, none of the techniques alone can give a complete picture of what is happening at the interface. Therefore, in this case, the structure and phases in the as-prepared state, as well as the various stages of reaction, have been characterized by XRD analysis and TEM observations.

It is seen that the nucleation of Ag_2Al phase takes place in the interface plane. The substrate plays a vital role in the phase formation; on NaCl substrate the growth is hindered. This might be due to the occurrence of fewer nucleation sites. Unlike Au/Al or Cu/Al, this system has relatively fewer phases, i.e. Ag_2Al and Ag_3Al, of which only Ag_2Al is detected. Generally, the phase having the lower free energy or negligible values of nucleation or growth rate should be the first formed. Unfortunately, these data are not available in the present case. However, the empirical rule [17] stating that the compound first formed is the congruent melting one, closer in composition to the lower temperature eutectic can be applied here to explain the formation of Ag_2Al phase.

The growth of the product phase takes place most probably by the diffusion of aluminium along the grain-boundary paths in Ag/Ag_2Al. There is a consequent change in resistivity because the resistivity of the product phase is higher than that of the components. Grain growth and precipitation of the product phase also probably occurs along the grain boundaries which subsequently spread along the whole grain, at least for the thicker films.

Acknowledgements

The authors thank the Polymer Science Unit, IACS, for assistance in DSC work and Professor S. P. Sengupta for his assistance in XRD work and keen interest in this work.

References

1. S. K. SEN, A. GHORAI, A. K. BANDYOPADHYAY and S. SEN, *Thin Solid Films* **155** (1987) 243.
2. R. J. HIGHMORE, J. E. EVETTS, A. L. GREER and R. E. SOMEKH, *Appl. Phys. Lett.* **50** (1987) 566.
3. K. R. COFFEY, L. A. CLEVENGER, K. BARMAK, D. A. RUDMAN and C. V. THOMPSON, *ibid.* **55** (1989) 852.
4. L. A. CLEVENGER, C. V. THOMPSON, R. C. CAMMARATA and K. N. TU, *ibid.* **52** (1988) 795.
5. J. E. E. BAGLIN, F. M. d'HEURLE and W. N. HAMMER, in "Procedings of the Symposium on Thin Film Phenomena, Interfaces and Interactions", edited by J. E. E. Baglin and J. M. Poate (1978) p. 171.
6. H. E. KISSINGER, *Anal. Chem.* **29** (1957) 1702.
7. L. A. CLEVENGER and C. V. THOMPSON, *J. Appl. Phys.* **67** (1990) 1325.
8. W. A. JOHNSON and R. F. MEHL, *Trans. AIME.* **135** (1939) 416.
9. M. AVRAMI, *J. Chem. Phys.* **7** (1939) 1103.
10. *Idem, ibid.* **8** (1940) 212.
11. *Idem, ibid.* **9** (1941) 177.
12. K. N. TU, W. K. CHU and J. W. MEYER, *Thin Solid Films* **25** (1975) 4031.
13. C. WEAVER and L. C. BROWN, *Phil. Mag.* **17** (1968) 881.
14. C. D. LIEN and M. A. NICOLET, *J. Vac. Sci. Technol.* **B2** (1984) 738.
15. E. MA, C. V. THOMPSON and L. A. CLEVENGER, *J. Appl. Phys.* **69** (1991) 2211.
16. S. MARDER and S. HERD, *Thin Solid Films* **10** (1972) 377.
17. R. M. WALSER and R. W. BENE, *Appl. Phys. Lett.* **28** (1976) 624.

Received 23 July 1991
and accepted 4 February 1992